Supporting Information

A simple design of vitrimer network with various fractions of bond exchangeable units for revisiting the Arrhenius dependence of relaxation properties

Taketo Isogai,[a] Mikihiro Hayashi*[a,b]

[a] Department of Life Science and Applied Chemistry, Graduate School of Engineering, Nagoya Institute of Technology, Gokiso-cho, Showa-ku Nagoya 466-8555, Japan
[b] PRESTO, Japan Science and Technology Agency, 4-1-8, Honcho, Kawaguchi, Saitama 332-0012, Japan

Corresponding: Mikihiro Hayashi (evh70675@ict.nitech.ac.jp)

1. Materials

Ethylene bis(thioglycolate) (SH-ester), 3,6-dioxa-1,8-octanedithiol (SH-ether), and 4,4′-methylenebis(*N,N*-diglycidylaniline) (4-Epoxy) were purchased from TCI. These chemicals were used as received.

2. Analytical methods

Swelling test

Swelling tests were carried out to estimate the swelling ratio (R_s) depending on the reaction time. The cross-linked samples (ca. 0.5 g) were immersed in the solvent (*N,N*-dimethylformamide, DMF), and R_s was estimated, according to $R_s = \frac{m_s}{m_i} \times 100$, where m_i and m_s is the initial and swollen mass, respectively. The gel fraction (ϕ_{gel}) was also estimated by the swelling test using tetrahydrofuran (THF). The solution was replaced with new solvent at an interval of 24 h for three times The final swollen samples were completely dried by vacuum, and the dried mass (m_d) was compared with m_i. The ϕ_{gel} was defined by the relationship, $\phi_{gel} = \frac{m_d}{m_i} \times 100$.

FT-IR spectroscopy

The reaction progress between the SH and epoxy groups was confirmed by Fourier transform infrared (FT-IR) spectroscopy. The measurements were performed at 25 °C using an FT/IR-4700 spectrometer combined with an ATR attachment (JASCO Co.). For the comparison of signals between the samples, the spectra were normalized focusing on the signal from phenyl rings of 4-Epoxy at ca. 1510 cm^{-1}.

Thermal properties

The glass transition temperatures (T_gs) of the obtained samples were investigated by differential scanning calorimetry (DSC), using a DSC7020 (Hitachi High-Tech). The second heating thermograms from -50 °C to 200 °C are provided in the text, where the temperature ramp rate was set to be 10 °C/min. The decomposition temperatures were determined using thermogravimetric analysis (TGA), a TG/DTA7300 (Hitachi High-Tech). The samples were heated from 30 °C to 500 °C at a temperature-ramp rate of 10 °C/min. All the above measurements were carried out using approximately 10 mg samples under N_2 gas environment.

Temperature-ramp rheology

The temperature-ramp rheology for the cross-linked samples was conducted, using a uniaxial rheometer DMS6100 (Hitachi High-Tech). For the measurements, rectangular-shaped samples with thickness of 1 mm, width of 4 mm, and length of 20 mm were prepared using a razor blade. The frequency and the strain was fixed to be 1 Hz and 0.05% (linear regime), respectively, for all samples. The temperature was increased from -40 °C to 200 °C at a temperature-ramp rate of 5 °C/min. The measurements were all performed under N_2 gas environment.

Temperature-ramp creep

The activation temperature of the bond exchange vitrimer (T_{act}) was evaluated via temperature-ramp creep tests, using a TMA7100 analyzer (Hitachi High-Tech). Rectangular-shaped samples with thickness of 1 mm, width of 4 mm, and length of 20 mm, were prepared using a razor blade. Constant small stress (50 kPa) was applied while increasing the temperatures at a ramp rate of 5 °C/min, where the changing behaviors of sample length was detected within the temperature range from 100 to 240 °C. The measurements were performed under N_2 gas environment.

Stress relaxation

The relaxation properties were investigated by stress relaxation tests, using a shear-type rheometer MCR102e (Anton Paar) and 8 mm parallel plates. Disc-shaped samples with diameter of 8 mm and thickness of 1 mm were prepared using a cutting die. The measurements were carried out at 160 °C, 170 °C, 180 °C, 190 °C, and 200 °C with an application of 5% strain (the linear regime was confirmed by strain-sweep tests). All measurements were conducted under N_2 gas environment. The tests were started after equilibration time of 30 min at each target temperature. To confirm the reproducibility of the data, measurements were conducted three times at each target temperature.

3. Variation of R_s and T_g depending on the reaction time

Variation of swelling ratio (R_s) and T_g depending on the heating time (t_r) were investigated for CL-100 and CL-0. R_s reached the minimum constant and T_g reached the highest constant after heating for 24 h. Therefore, the necessary heating time for the optimization was determined to be 24 h. Note that the conversion of the reacting groups (i.e., thiol and epoxy) were confirmed by FT-IR in the following section.
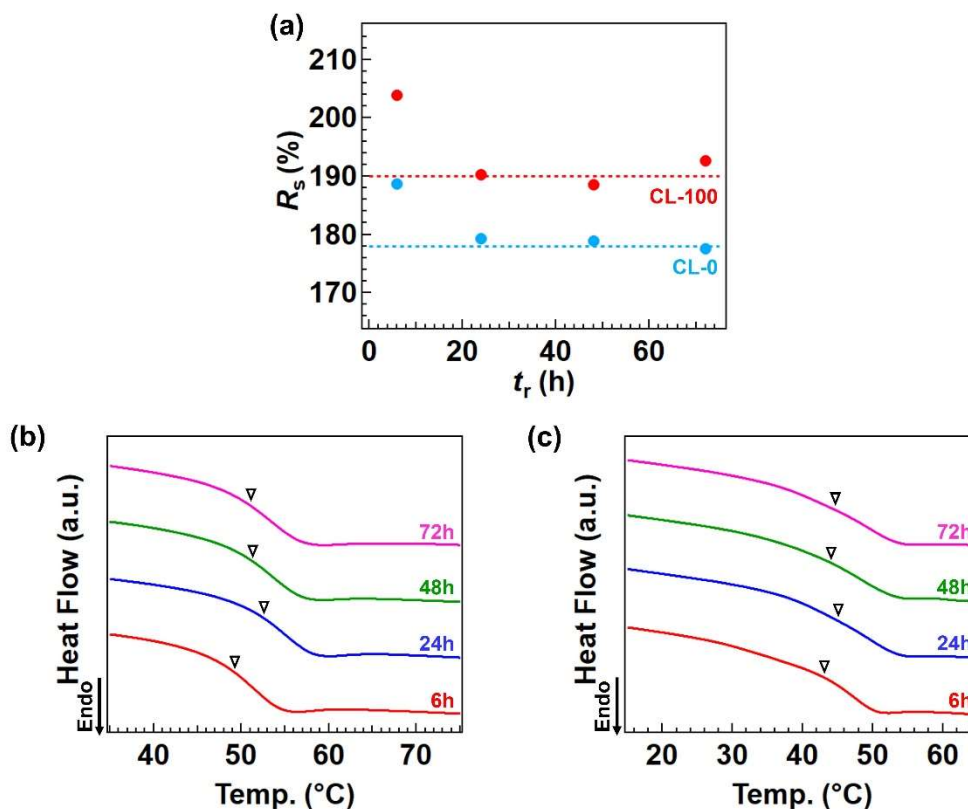

Figure S1. (a) Variation of R_s as a function of reaction heating time (t_r) and the corresponding DSC thermograms for (b) CL-100 and (c) CL-0.

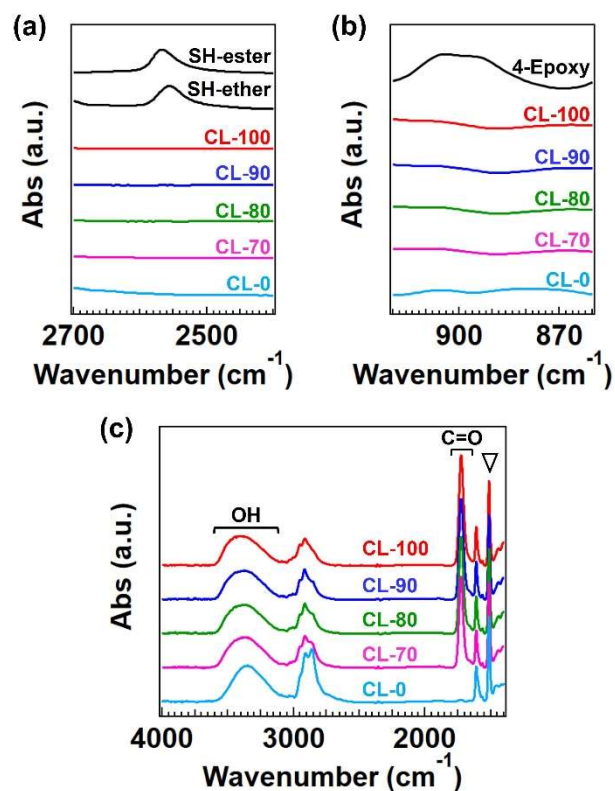## 4. FT-IR data for confirmation of reaction

Figure S2. FT-IR spectra for the cross-linked samples at (a) 2400 to 2700 cm^{-1}, (b) 860 to 920 cm^{-1}, and (c) 1400 to 4000 cm^{-1}. In (c), the inverse triangle symbol represents the position of the phenyl ring signal used for the normalization.

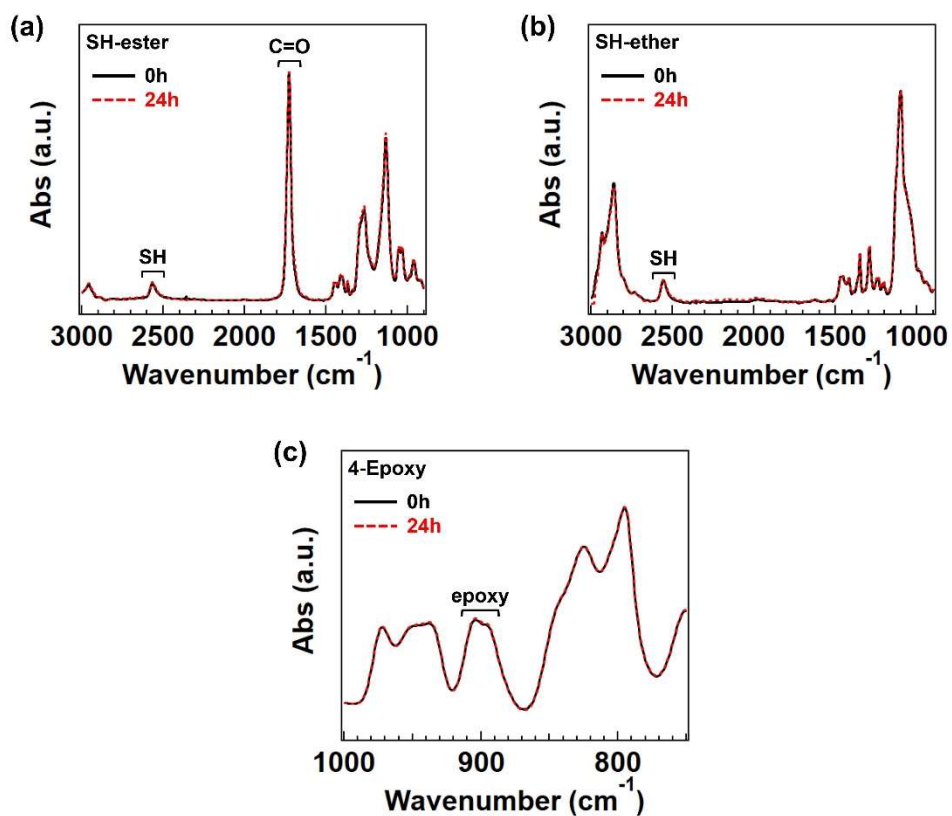**5. FT-IR data of the component monomers after long time heating**

Figure S3. FT-IR data of (a) SH-ester, (b) SH-ether, and (c) 4-Epoxy after heating treatment at 120 °C for 24 h, where the spectra at the initial state are also shown for comparison.
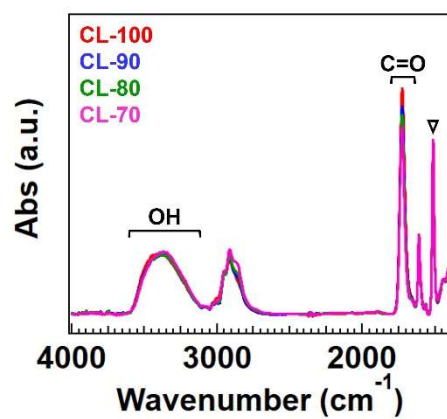
6. Overlaid FT-IR spectra

Figure S4. Overlaid FT-IR spectra for the cross-linked samples, where the spectra were normalized by the signal of phenyl ring of 4-Epoxy at 1510 cm^{-1}.
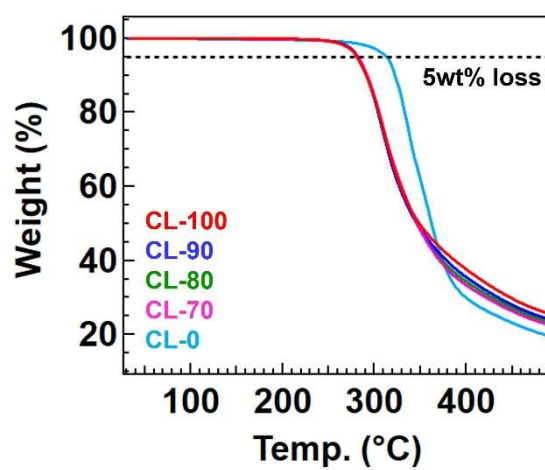
7. TGA thermograms

Figure S5. TGA thermograms for the cross-linked samples. The dotted line indicates the 5% weight loss.

8. Temperature-ramp creep

Figure S6 provided the creep behaviors of CL-100 and CL-0, where the Y-axis represents the sample length (L) normalized at the length at 100 °C ($L_{100°C}$). For CL-100, the experimental curve (solid curve) was clearly deviated from the extrapolated straight line from the low temperature (broken line), showing the creep behavior. On the other hand, such a deviation was not observed for CL-0. Because CL-0 with no ester bonds did not show the creep, the observed creep for CL-100 was assumed to be due to the bond exchange via transesterification, and T_{act} was determined to be ca. 150 °C - 160 °C for the present system.
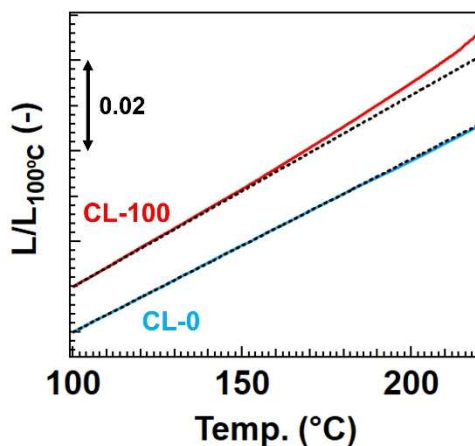

Figure S6. Temperature-ramp creep data for CL-100 and CL-0. The Y-axis represents the sample length (L) normalized at the length at 100 °C ($L_{100°C}$). The experimental data are provided by the solid curves, whereas the dotted lines represent the approximation straight lines extrapolated from low temperature regions.

9. Reproducibility of stress relaxation data

Figure S7 summarized the representative examples of reproducibility of stress relaxation data for CL-100 measured three times at each temperature. The reproducibility was also confirmed for other samples at different temperatures.
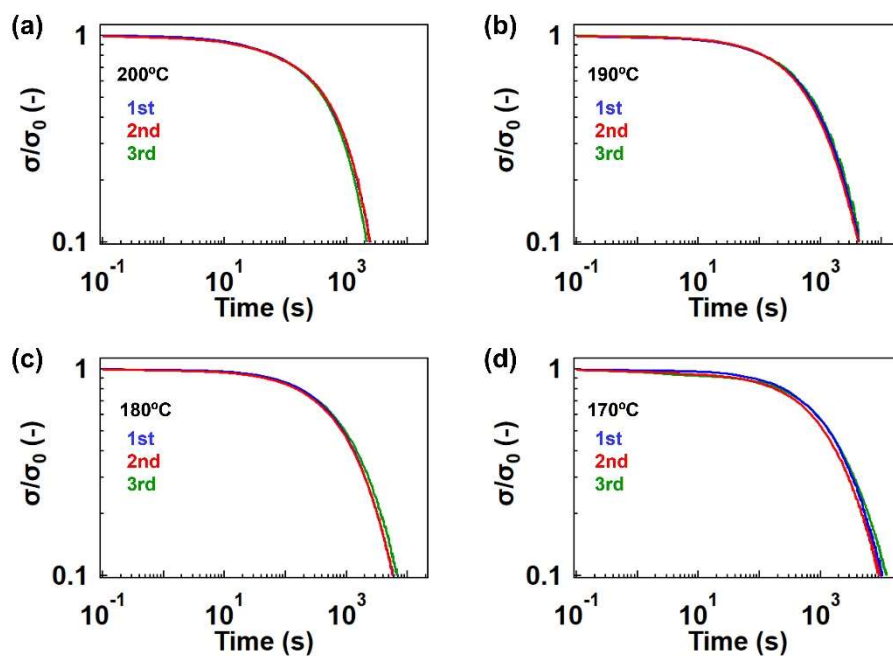

Figure S7. Reproducibility of stress relaxation data measured for CL-100 as a representative example at (a) 200 °C, (b) 190 °C, (c) 180 °C, and (d) 170 °C.

10. Long time stress relaxation data for CL-100

The stress relaxation test was measured for CL-100 as a representative sample at 200 °C until the normalized stress was decreased to be 0.01 of the initial stress.
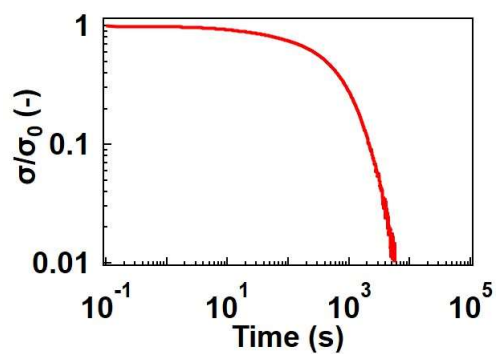

Figure S8. Long time stress relaxation data for CL-100 measured at 200 °C.

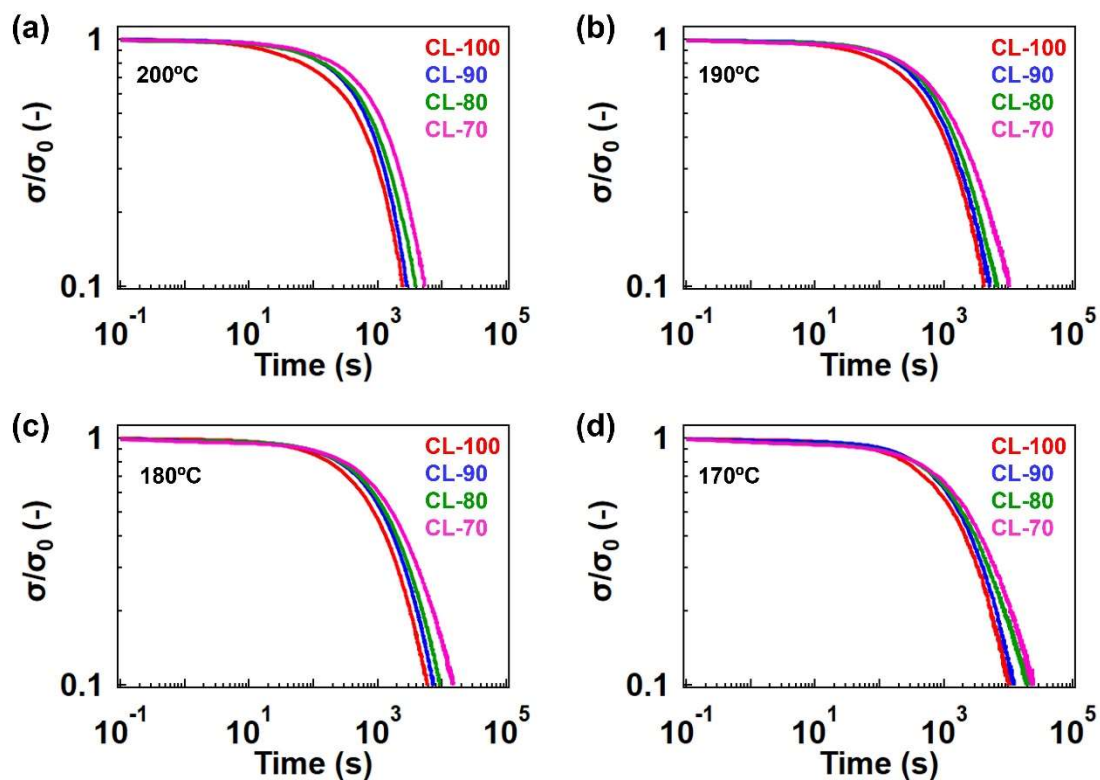## 11. Comparison of stress relaxation data at various temperatures

Figure S9. Comparison of stress relaxation data at (a) 200 °C, (b) 190 °C, (c) 180 °C, and (d) 170 °C.

12. Stress relaxation data for CL-60 and CL-50

To confirm the vaiildity of the inverse propertionality between the relaxation time and f_{ester} for the samples with a smaller fraction of ester units, we prepared other samples, CL-60 and CL-50. The representative data at 170 °C were shown in Figure S10a and S10b. From the fitting process, the values of $<\tau>$ was estimated, and the plots were added in Figure S10c. The inverse propertionality observed for samples with f_{ester} of 70 - 100 did not hold for CL-60 and CL-50, where $<\tau>$ for CL-60 and CL-50 was much larger (and thus $1/<\tau>$ was much smaller) than the expected values. The interpretation of this deviation is provided in the the last part of the main text.
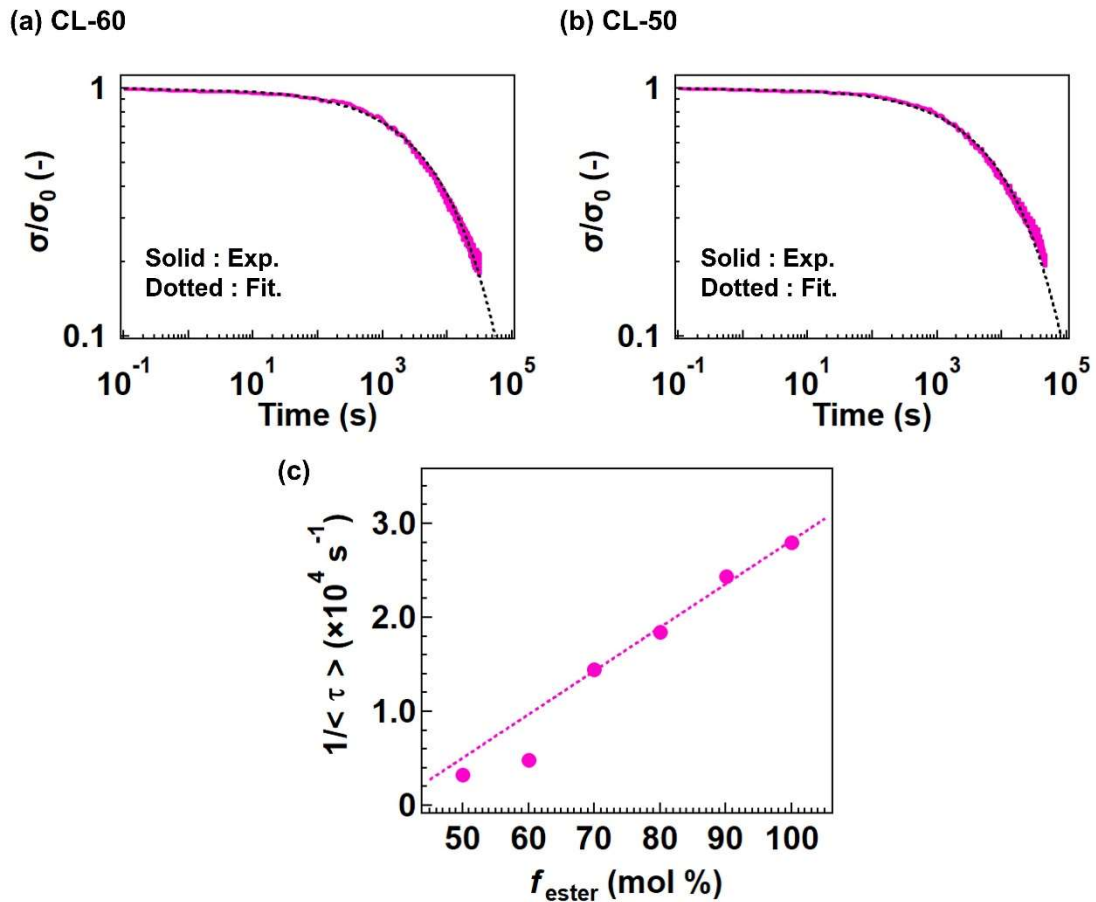

Figure S10. Stress relaxation curves for (a) CL-60 and (b) CL-50 at 170 °C. The Y-axis indicates the stress (σ) normalized by the initial stress (σ_0). The dotted curves represent the fitting curves based on the KWW function. (c) Plots of inverse $<\tau>$ as a function of f_{ester} within the f_{ester} range of 50 - 100.

13. Stress relaxation data at 160 °C

The stress relxation was perfomed at 160 °C. For CL-70 and CL-80, the plot of $<\tau>$ at 160 °C was deviated from the Arrhenius dependence derived for the data taken at 170 - 200 °C.
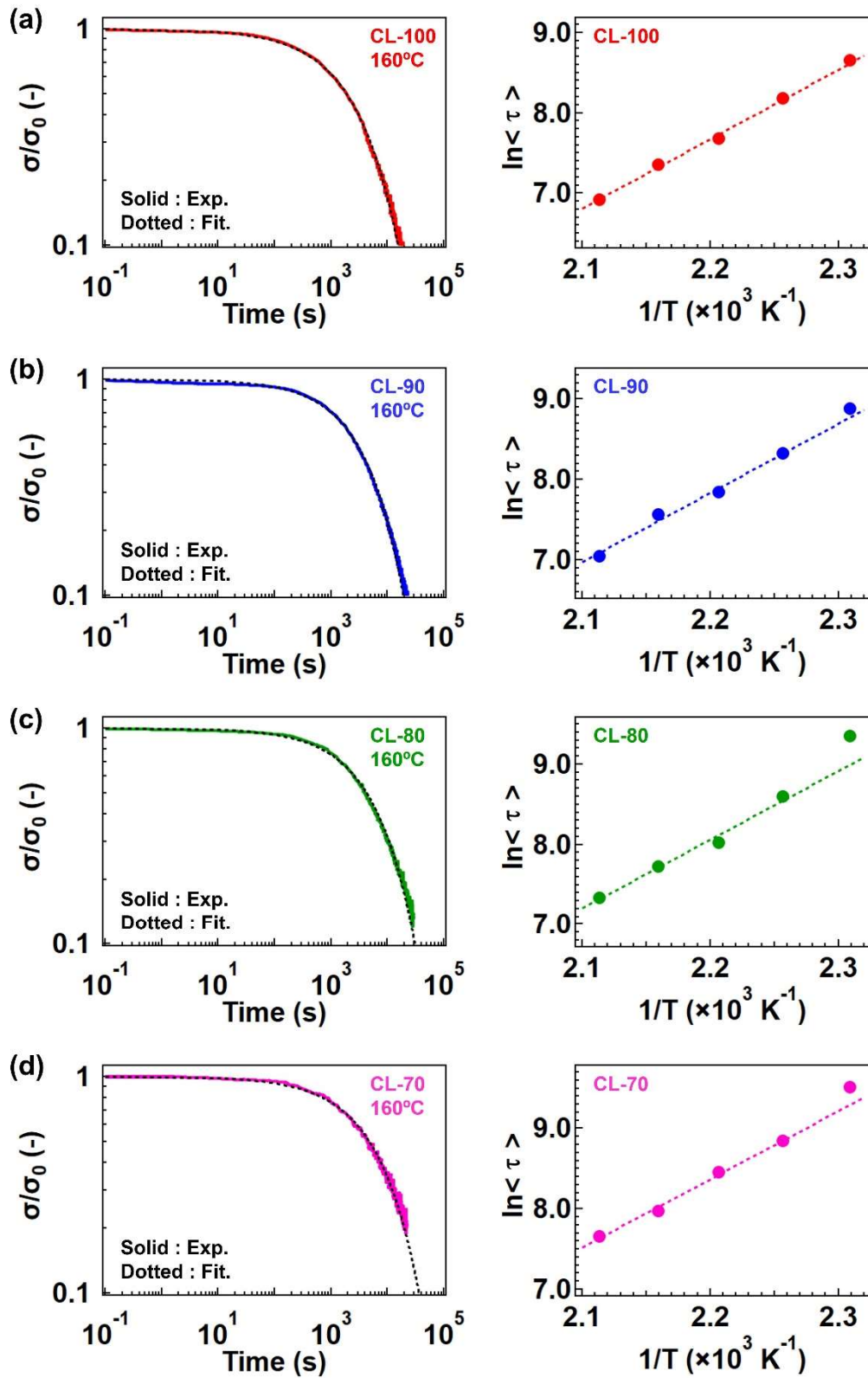

Figure S11. Stress relaxation curves and temperature dependence of $<\tau>$ for (a) CL-100, (b) CL-90, (c) CL-80, and (d) CL-70 at 160 °C.